

Morphology of Alloy Elements and Electrochemical Effects of $\text{Li}_4\text{Ti}_5\text{O}_{12}$ /Graphene Produced by Ball Milling

C.G. Nava-Dino¹, R.G. Bautista-Margulis^{2,*}, J.E. Mendoza-Negrete³, G. Llerar-Meza¹, J.P. Flores de los Rios⁴, G. López-Ocaña², M.I. Ferrer-Sánchez², J.G. Chacón-Nava⁴, A. Martínez-Villafañe⁴

¹Universidad Autónoma de Chihuahua, Facultad de Ingeniería, Circuito No. 1., Campus Universitario 2. Chihuahua, Chih., C.P. 31125, México.

²Universidad Juárez Autónoma de Tabasco, División Académica de Ciencias Biológicas, Villahermosa-Tabasco, C.P. 86040, México.

³Universidad Autónoma de Chihuahua, Facultad de Filosofía y Letras, Rúa de las Humanidades s/n, Campus Universitario I. Chihuahua, Chih., C.P. 31125, México.

⁴Departamento de Integridad y Diseño de Materiales Compuestos. Centro de Investigación en Materiales Avanzados, Miguel de Cervantes No. 120, Complejo Industrial Chihuahua, C.P. 31109, Chihuahua, Chih., México.

*E-mail: margulisrg@hotmail.com

Received: 23 January 2015 / Accepted: 10 March 2015 / Published: 23 March 2015

In the past two decades, many researchers focused their attention on metallic or semi-metallic elements which can alloy with lithium reversibly and release a high Li-storage capacity. The research samples of $\text{Li}_4\text{Ti}_5\text{O}_{12}$ /Graphene at hand were made with mechanical ball-milling technique (MA). Drops of graphene oxide were added to the powder of $\text{Li}_4\text{Ti}_5\text{O}_{12}$, and thus enhanced the structural stability of the alloying. The main idea is to build a work electrode suitable for electrochemical test to be used in storage batteries. In order to deeply understand the behavior of graphene reaction in lithium, scanning electron microscopy (SEM) images were analyzed using algorithms from digital processing images. A complete characterization of alloying was also made, including X-Ray, transmission electron microscopy (TEM) and electrochemical noise (EN).

Keywords: Mechanical Alloying, Energy Storage Materials, Powder Metallurgy, Electrochemical Noise, Computer Simulations.

1. INTRODUCTION

Graphitic structured materials like carbon nanotubes (CNTs) and graphene have been among the most widely researched materials due to their exceptional mechanical, thermal, and electrical properties, and their tribological behavior. Moreover, improved manufacturing techniques have made

these materials more affordable [1-2]. Other studies tried with Li_2TiO_3 /Reduced Graphene Oxide composite and were synthesized with (LTO) and graphene oxide nanosheets by spray-drying and annealing processes [3-4].

The high energy density of LIBs (Li-ion battery) has been produced, but the low rate capability of LIBs has been limited. High power density and long cycle life are urgently required. Among various anode materials for LIBs, $\text{Li}_4\text{Ti}_5\text{O}_{12}$ has been intensively investigated for its excellent cycling [5]. Graphene oxide (GO) in nature inherits the 2D carbon backbone from graphene [6]. The states of the art in cathodes of rechargeable lithium ion batteries are transition metal oxides. Typically oxides are being explored as cathode materials where the oxide anion forms a weak ligand. Some investigations use manganese ferrocyanide as cathode candidate combined with graphene nanosheets by mechanical ball-milling [7]. In this research droops of graphene oxide were mixed with Li_2TiO_3 and $\text{Li}_4\text{Ti}_5\text{O}_{12}$, finding a better alloying using $\text{Li}_4\text{Ti}_5\text{O}_{12}$ /Graphene.

Several studies used SEM and TEM to understand changes in morphology, results indicates that graphene oxide could be reduced after ball milling. Meanwhile, the electrochemical properties of such graphene as electrode materials were obviously enhanced [8-9].

Graphene has attracted unprecedented scientific and technological interest due to its unique electrical and mechanical properties in a short span of time [10]. Some studies handle ball milling is a widely used method to improve properties for preparation and after treatment of several materials such as activated carbon. In order to increase the lithium density in this investigation ball milling was used by mixing graphene oxide. Another way to increase the performance of Spinel $\text{Li}_4\text{Ti}_5\text{O}_{12}$, was synthesized and characterized as anode materials by ethanol-assisted hydrothermal synthesis [11]; any way the several techniques to improve Li density needs a lot of laboratory requirements. To reduce laboratory test and resources in this study, MATLAB software was used as a computer tool to evaluate images, obtained by TEM. These images allow analyzing and predicting the behavior of the samples.

Another analysis of $\text{Li}_4\text{Ti}_5\text{O}_{12}$ /TiN nanocomposites fabricated through high energy ball-milling of the mixture of spinel, show that all ball milled samples exhibit markedly improved electrochemical properties in comparison with $\text{Li}_4\text{Ti}_5\text{O}_{12}$ [12]. High-resolution electron microscopy is an efficient tool for characterizing heterogeneous nanostructures; however, currently the analysis is a laborious and time consuming manual process [13-14]. Applications of digital image processing techniques permits extract meaningful structural descriptors from the acquired images [15].

2. EXPERIMENTAL PROCEDURE

2.1 Preparation of Nanopowders by MA

Pure materials from Sigma Aldrich: Lithium Titanate Spinel (99.0% purity), Lithium Titanate Oxide, and Graphene Oxide 2Mg/ML dispersion in H_2O powders were used. SPEX 8000M was connected to a hardened steel container with 13 mm (\varnothing) balls as milling media and an inert Ar atmosphere. The milling ball to powder weight ratio was kept 5 to 1 for all experimental runs. Milling intervals were 0, 4 and 8 hrs. using alternate cycles of 30 minutes milling and 30 min resting.

Table 1 shows density picometer of powders, density change with milling time. Density increases with graphene added and could be decreased with influence of milling time. Figure 1 shows the TEM images 0 and 8 hrs. In Fig.1 a) it is clearly observed the hexagons shape made by graphene at 0h. These geometric structures are de ROI (Region Of Interest) analyzed in this research. Microstructural observations were performed by SEM (JEOL-5800-LV) and TEM (Philips JEM-2200FS) equipped with energy dispersive spectrometer (EDS).

Table 1. Density of powders $\text{Li}_4\text{Ti}_5\text{O}_{12}$ with and without Graphene.

| Density without Graphene | Density with Graphene | Milling Intensity [h] SPS |
|--------------------------|-----------------------|---------------------------|
| 4.4864 g/cc | 4.5902± 1.082 g/cc | 0h |
| 4.904 ± 0.61 g/cc | 5.7434 ± 1.082 g/cc | 4h |
| 4.7856 ± 0.341 g/cc | 3.7107 ± 0.054 g/cc | 8h |

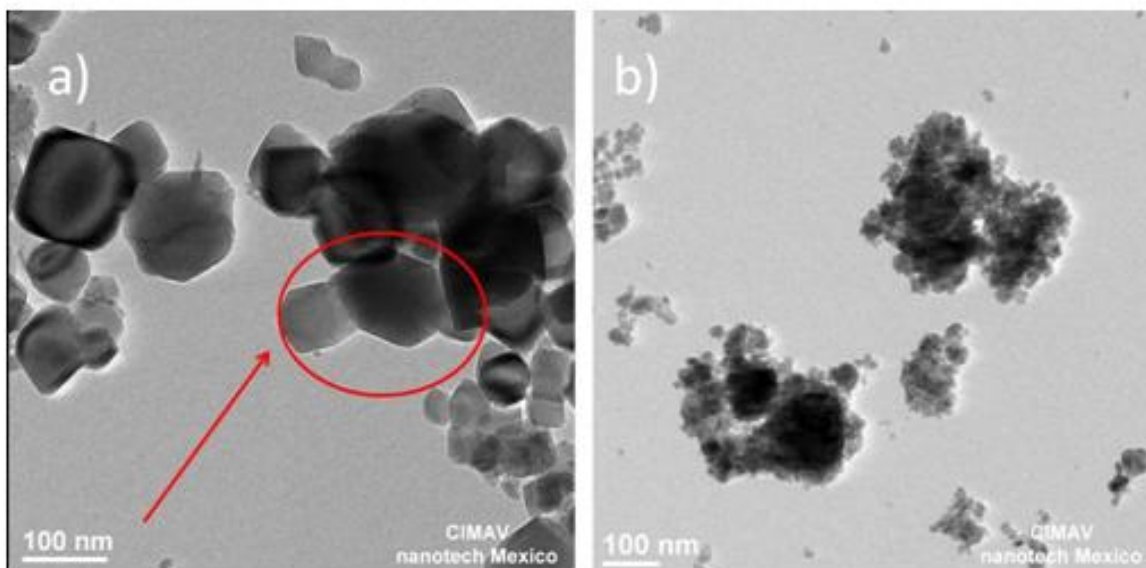


Figure 1. TEM images of $\text{Li}_4\text{Ti}_5\text{O}_{12}$ /Graphene at a) 0h and b) 8h of alloying.

2.2 Image Processing

Mathematical morphology offers popular image processing tools, successfully used for binary and grayscale images. The gray scale morphology is based on the lattice theory, which implies a partial ordering of the data within the grayscale images [16-17]. Image segmentation plays a very important role in computer vision and artificial intelligence. Its goal is to extract ROI from a given image.

2.3 Theory/calculation

MATLAB provides a powerful internal function for high-performance numerical computation and visualization. Using MATLAB's *imread* function was readable into matrix from the TEM images. Pixel is used to denote the spatial element of a digital image. The size of a digital image can be denoted as $M \times N$, where M is the number of pixel columns (width) and N is the number of pixel rows (height). The clarity of a TEM image is determined by spatial resolution in pixels per nanometer, not just the number of pixels in an image.

A negative transformation is applied after the program loads an eight-bit grayscale TEM image to be processed. The negative transformation can be expressed as:

$$I_{negative} = L - I - I_{original} \quad (1)$$

where L is the number of discrete intensity levels (256 for the sample of $\text{Li}_4\text{Ti}_5\text{O}_{12}$ /Graphene image); $I_{original}$, the values of pixels before transformation; and $I_{negative}$, the values of pixels after transformation.

2.4 Electrochemical Test

The tests were made in ACM Instruments Gill AC. The electrodes of $\text{Li}_4\text{Ti}_5\text{O}_{12}$ and Li_2TiO_3 were coated with epoxy resin and then were rinsed in sodium hydroxide (NaOH) solution. Samples were immersed in NaOH solution for 15 minutes of stabilization and the open circuit potential was measured during this period with a multimeter; the OCP samples were -195 and -175 mV vs SCE. All tests were performed at room temperature; analysis was carried out according to ASTM G1 and G199. The statistical analysis was achieved in time intervals of 1024 seconds. The time intervals were selected from the last section from the records, where stabilization was reached.

3. RESULTS AND DISCUSSION

The first objective in this study was to understand milling time. Long ball milling time is not beneficial for the electrochemical properties; in this research 10h of ball milling can pollute samples. For other studies when the ball milling time reaches 50 h, the capacitance sharply decreases and it is very likely to find re-oxidation of samples [18]. In figure 2, X-ray diffraction pattern of the $\text{Li}_4\text{Ti}_5\text{O}_{12}$ samples at 0, 4, 8 h are show. A Panalytical X'Pert PRO diffractometer (40 kV, 35mA) with Cu $K\alpha$ radiation ($\lambda = 0.15406$ nm) was used for the measurements. In order to identify Lithium, an IEES (Electron Energy Loss Microscopy) analysis was carried out (Figure 3). The peaks of Lithium can be compared with the references observed in EELS Atlas made by Burgner [19-20], combining with EELS techniques to identify oxide states and charge distributions, in situ TEM may expand applications in the study of cathode materials [21-22-23].

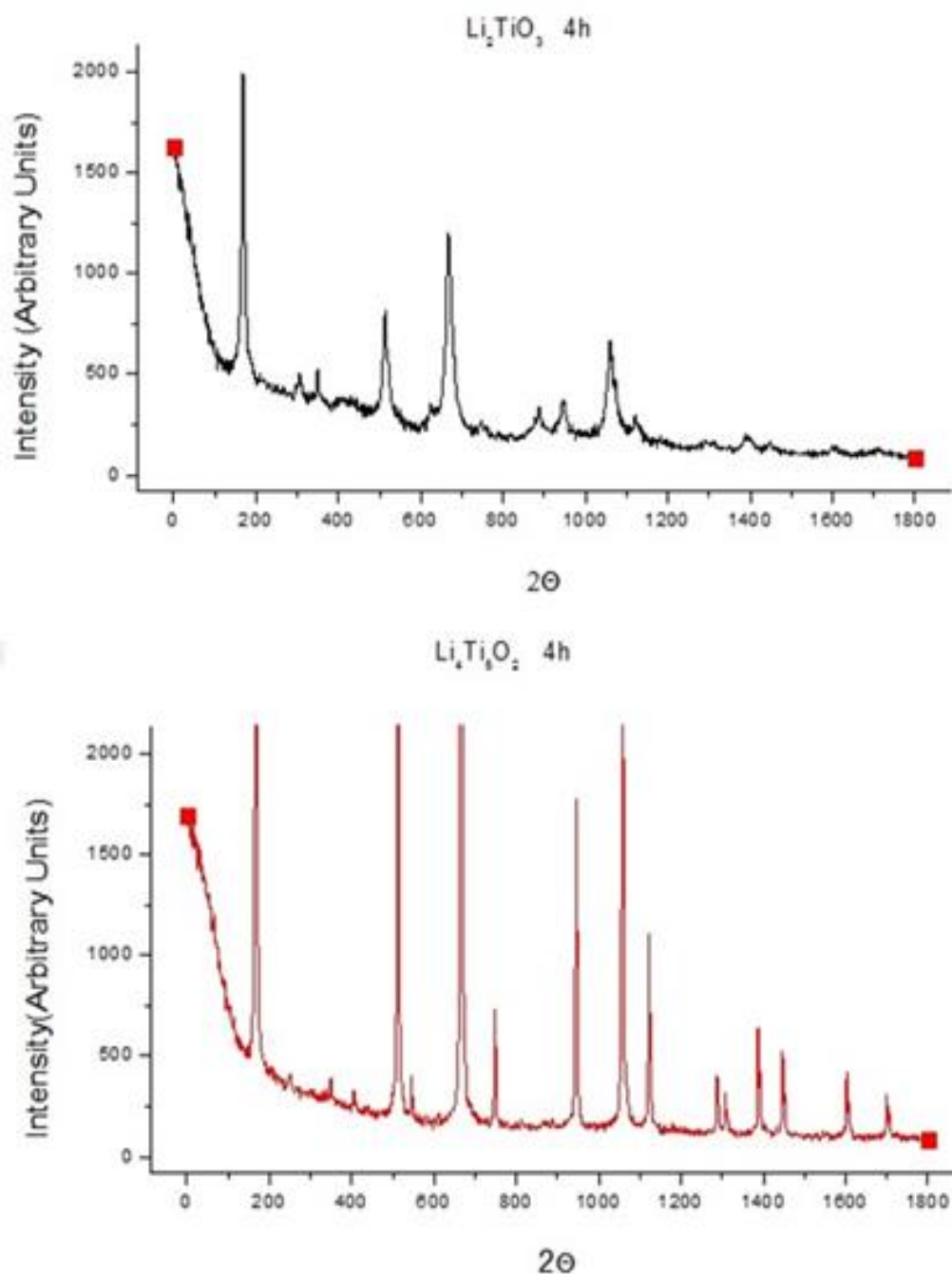


Figure 2. X-ray diffraction pattern of the $\text{Li}_4\text{Ti}_5\text{O}_{12}$ samples at 4 h.

Transmission electron microscopy (TEM) investigations provides structural and compositional information with nanoscale spatial resolution and subsecond temporal resolution, to understand the dynamic structural evolution of the whole anode, which is essential for understanding the behavior of materials in the electrode HRTEM which, in turn, allows observation for the geometrical and structural behavior of the anode samples. Figure 4d shows the negative image of the original HRTEM image (Fig. 4a) obtained using the negative transformation in Eq. (1).

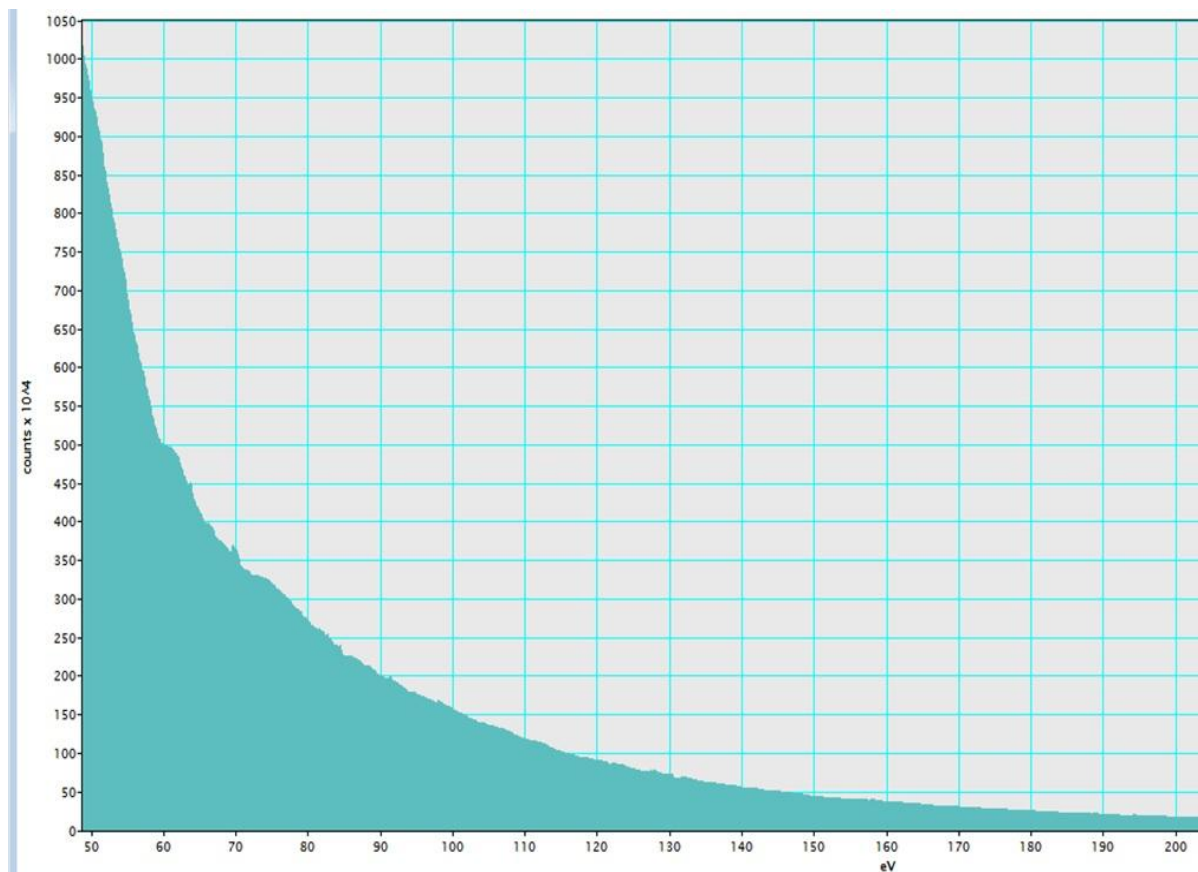


Figure 3. IEES analysis for Lithium detection.

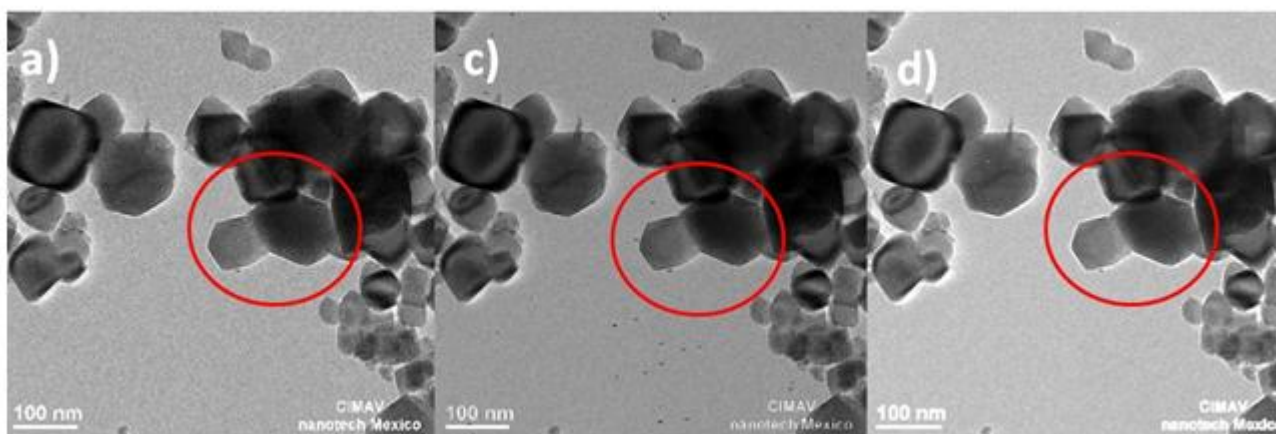


Figure 4. TEM images processing show the graphene layers within the red circle.

The algorithm permits the user to select a region of interest (ROI) as shown in Fig. (5a) for further processing (Fig. 5e). Figure (5b) was obtained by forcing pixels outside the ROI of Fig. (5a) to

the lowest intensity level. The ROI should consist of the region(s) that contain sufficient and clear fringe information.

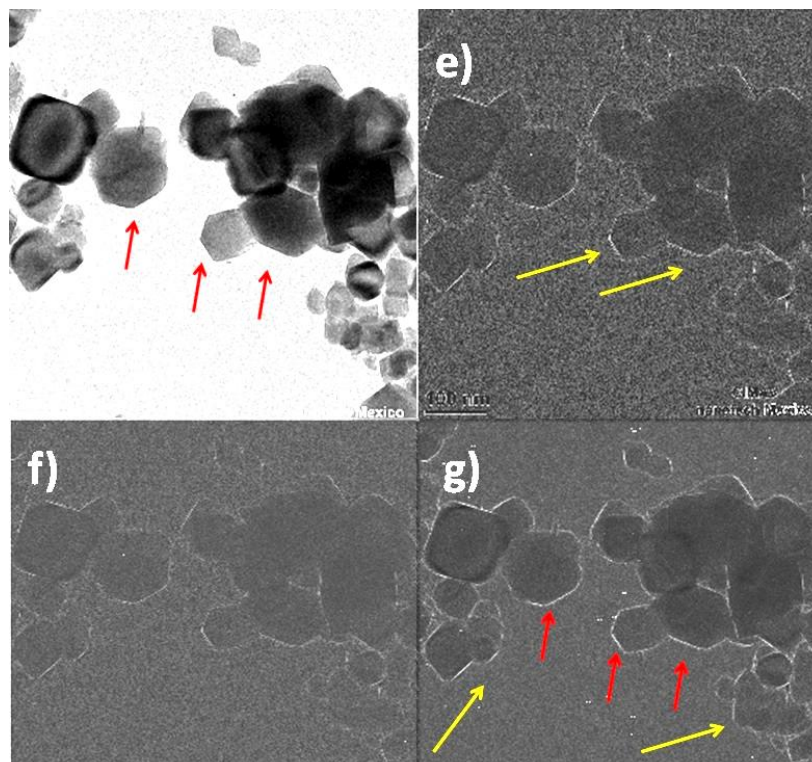


Figure 5. New fringes are observed after images processing in g).

The images process technique allows the quantification of the carbon structure of samples and graphene layers. The behavior of Lithium in this research was studied with IEES using a TEM microscopy. Observing graphene and Lithium was a complicated activity; to select this alloying as a good cathode or anode, image processing could be a good alternative; but resolution and differences between fringes made it possible to carry on the research. Results of electrochemical activity were made by Electrochemical Noise technique (EN), as shown in figure 5 for Li_2TiO_3 and figure 6 for $\text{Li}_4\text{Ti}_5\text{O}_{12}$. Electrochemical noise (EN) technique is one of the most promising methods for monitoring and studying corrosion processes [24]. Furthermore, EN technique was selected because of its importance to re-oxidation during milling process.

EN and image analysis was studied with different tools as a fuzzy sets and a fractal geometry [25], EN data of different corrosion systems and multifractal analysis from images of corroded surfaces has not been explored [26], but it is known that EN data and images of corroded surfaces in different media have a correlation. Figures 6 and 7 illustrate the average of samples of $\text{Li}_2\text{TiO}_3/\text{GO}$, $\text{Li}_4\text{Ti}_5\text{O}_{12}/\text{GO}$, where the electrochemical behavior with Lithium Spinel presented a better response than Lithium Titanate Oxide.

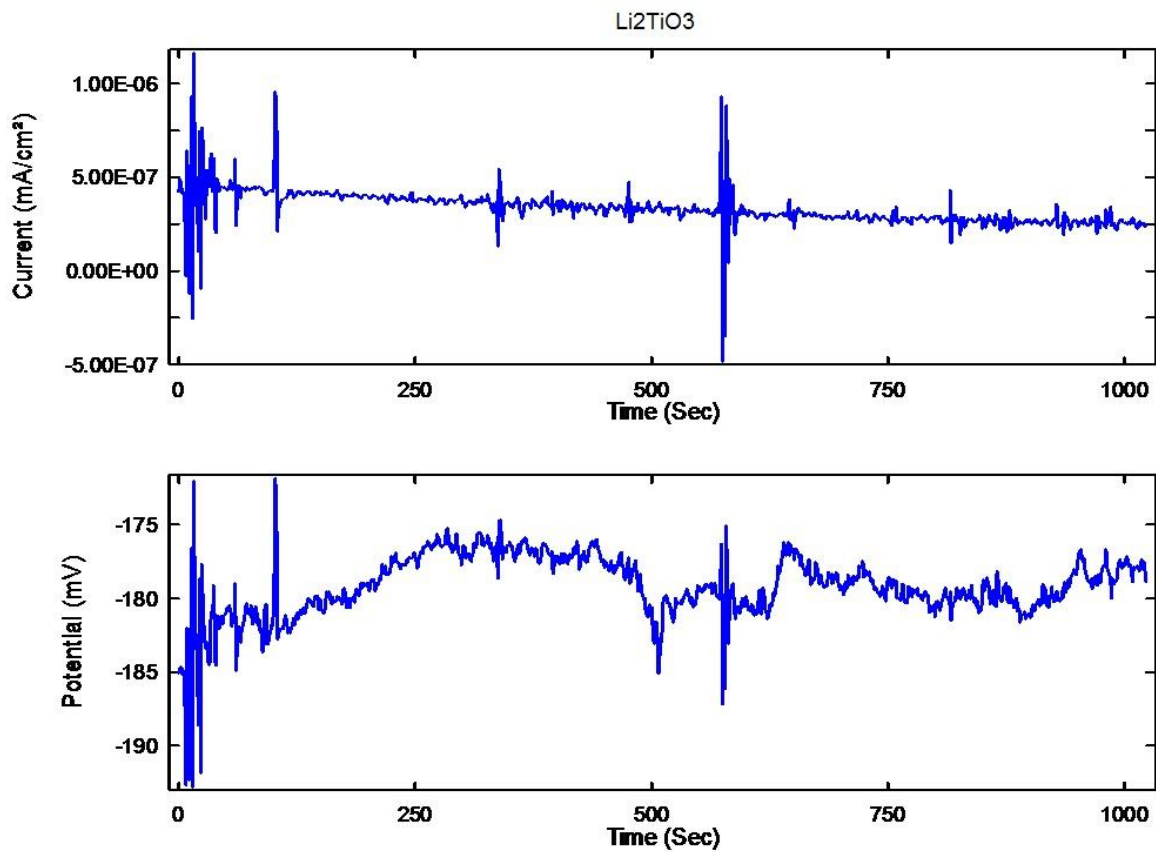


Figure 6. Electrochemical performance of Li_2TiO_3/GO .

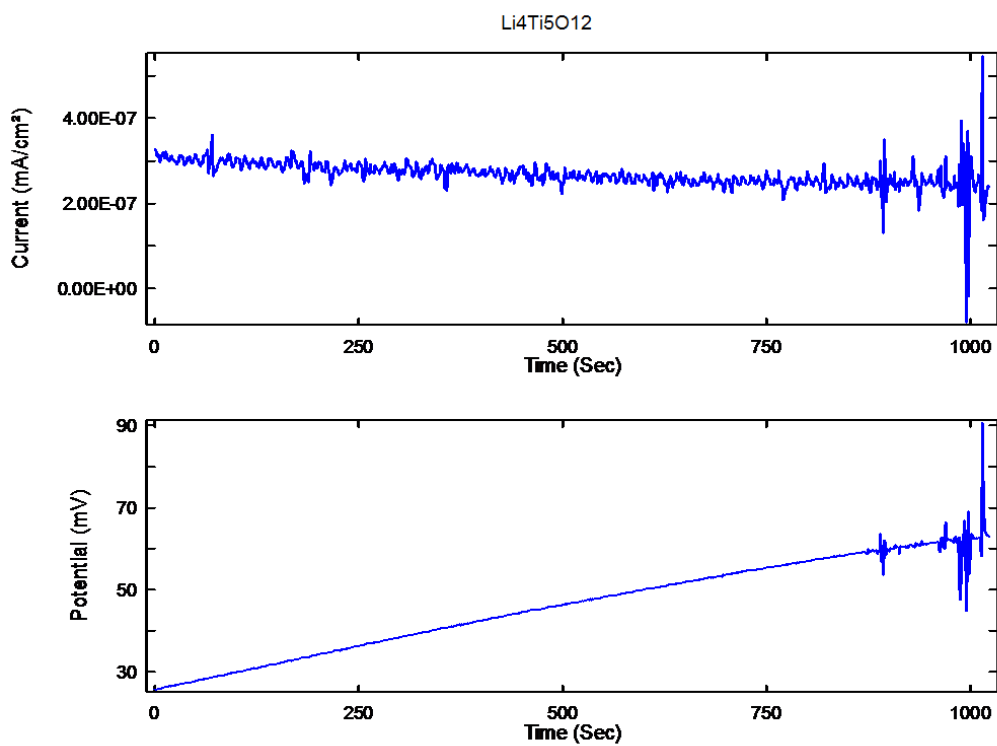


Figure 7. Electrochemical performance of $Li_4Ti_5O_{12}/GO$.

4. CONCLUSIONS

➤ In this research work, science tools materials were used and combined with digital processing images to find a good cathode/anode electrode capable of working as the main element for batteries design. Technical limitations to observe graphene, as an X-ray diffraction and Raman spectroscopy, prompted this investigation to develop materials for energy storage. The current results clearly demonstrated that image analysis processes were highly quantifiable and it could be consistently processed using a complete set of processing parameters.

➤ Electrodes were successfully performed adding graphene. Ball milling time was dependent on the injected quantity of milling energy. Differences between 4h and 8h were noticeable.

➤ A great number of high quality micrographs were necessary to obtain a reliable analysis and quantification of materials with heterogeneous structures, as well as to find out the relationship with electrochemical activity and the geometrical structures of the samples.

➤ The applications of graphene oxide (GO) for the electrochemical activity were satisfactorily demonstrated. Nevertheless, further investigation of advanced electrochemical techniques is still needed to be used in energy storage.

ACKNOWLEDGEMENTS

This research work was supported by PROMEP #OF-13-7029-UACH-PTC-291. The technical assistance by Adan Borunda Terrazas, Jair M. Lugo Cuevas, Gregorio Vazquez Olvera, Zohaila Azar, Vanessa Espejel and Leticia Mendez Mariscal is gratefully acknowledged.

References

1. A.M. Pinto, I.C. Goncalves, F.D. Magalhães. *Colloids and Surfaces B: Biointerfaces*, 111(2013) 188-202.
2. Mina Bastwros, Gap-Yong Kim, Can Zhu, Kun Zhang, Shiren Wang, Xiaoduan Tang, Xinwei Wang. *Composites: Part B* 60, (2014) 111-118.
3. Qian Zhang, Wenjie Peng, Zhixing Wang, Xinhai Li, Xunhui Xiong, Huajun Guo, Zhiguo Wang, Feixiang Wu. *Solid State Ionics*, 236 (2013) 30-36.
4. Zhongxue Chen, Kai Xie, Xiaobin Hong. *Electrochimica Acta*, 108 (2013) 674-679.
5. Qian Zhang, Wenjie Peng, Zhixing Wang, Xinhai Li, Xunhui Xiong, Huajun Guo, Zhiguo Wang, Feixiang Wu. *Solid State Ionics*, 236 (2013) 30-36.
6. Ling Sun, Bunshi Fugetsu. *Chemical Engineering Journal*, 240 (2014) 565-573.
7. Xiao-Jun Wang, Frank Krumeich, Reinhard Nesper. *Electrochemistry Communications*, 34 (2013)246-249.
8. Dacheng Zhang, Xiong Zhang, Xianzhong Sun, Haitao Zhang, Changhui Wang, Yanwei Ma. *Electrochimica Acta*, 109 (2013) 874-880
9. Ming Hong, Yingchun Zhang, Yingying Mi, Maoqiao Xiang, Yun Zhang. *Journal of Nuclear Materials*, 445 (2014) 111-116
10. Shin-Liang Kuo, Wei-Ren Liu, Chia-Pang Kuo, Nae-Lih Wu, Hung-Chun Wu. *Journal of Power Sources*, 244 (2013) 552-556.

11. Ting-Feng Yia, Shuang-YuanYang, Yan-RongZhu, Ming-FuYe, YingXie, Rong-Sun Zhu. *Ceramics International*, Volume 40, Issue 7, Part A, August 2014, pp. 9853–9858.
12. Jiwei Zhang, Jingwei Zhang, Wei Cai, Fenli Zhang, Laigui Yu, Zhishen Wu, Zhijun Zhang. *Journal of Power Sources*, 211 (2012) 133-139.
13. P. Toth, J.K.Farrer, A.B.Palotas, J.S.Lighty, E.G.Edding. *Ultramicroscopy*, 129 (2013) 53-62.
14. Lewys Jones, Peter D. Nellist. *STEM*, Volume 63, August 2014, pp. 47-51.
15. Yamamoto S., Matsunaga T., Nakamura R., Sekine Y., Hirata N., Yamaguchi Y. *Geoscience and Remote Sensing, IEEE Transactions on Volume: 53, Issue: 2* DOI: 10.1109/TGRS.2014.2327121.
16. Alexandru Căliman, Mihai Ivanovici, Noël Richard. *Pattern Recognition*, 47(2014)721-735.
17. Qiang Zheng, En-Qing Dong. *Acta Automatica Sinica*, 2013, Vol. 39, No. 1.
18. R. Parviz, R.A. Varin. *International Journal of Hydrogen Energy*, 3 8 (2013) 8313-8327.
19. Mitsuharu Tabuchi, Mitsunori Kitta, Hiroyuki Kageyama, Hideka Shibuya, Junichi Imaizumi. *Journal of Power Sources*, 279 (2015) 510-516.
20. Zongyuan Wang, Chang-JunLiu, *Nano Energy* (2015) 11, 277-293.
21. Su-Yuan Yan, Cheng-Yang Wang, Rong-Min Gu, Shuai Sun, Ming-Wei Li, *Journal of Alloys and Compounds* (2014), doi: <http://dx.doi.org/10.1016/j.jallcom.2014.12.182>.
22. Minhua Shao. *Journal of Power Sources*, 270 (2014) 475-486.
23. FanWu, NanYao. *Nano Energy*, (2015) 11, 196-210.
24. M. Shahidi1, H. Tajabadipour, H. Ganjalikhan Hakemi, M.R. Gholamhosseinzadeh. *Int. J. Electrochem. Sci.*, 8 (2013) 11734-11751.
25. Li Jian, Kong Weikang, Shi Jiangb2, Wang Ke, Wang Weikui, Zhao Weipu, Zeng Zhoumo. *Int. J. Electrochem. Sci.*, 8 (2013) 2365-2377.
26. W. Sanchez-Ortiz, C. Andrade-Gómez, E. Hernandez-Martinez, H. Puebla. *Int. J. Electrochem. Sci.*, 10 (2015) 1054-1064.